This full text paper was peer reviewed at the direction of IEEE Communications Society subject matter experts for publication in the IEEE Globecom 2010 proceedings.

# An Reformulation-Linearization Technique-based Approach to Joint Topology Design and Load Balancing in FSO Networks

In Keun Son and Shiwen Mao
Department of Electrical and Computer Engineering, Auburn University, Auburn, AL
Email: soninkeun@auburn.edu, smao@ieee.org

***Abstract*—Free space optical networks have emerged as a viable technology for broadband wireless backbone networks. In this paper, we investigate the challenging problem of joint topology design and load balancing in FSO networks. We consider FSO link characteristics, cost constraints, traffic characteristics, traffic demand, and QoS requirements in the formulation, along with various objective functions including network-wide average load and delay. We apply the Reformulation-Linearization Technique (RLT) to obtain linear programming (LP) relaxations of the original complex problem, and then incorporate the LP relaxations into a branch-and-bound framework. The proposed algorithm can produce highly competitive solutions with performance guarantees in the form of bounded optimality gap. The RLT-based branch-and-bound algorithm is evaluated with extensive simulations and is shown to be highly suitable for jointly optimizing topology and load balancing in FSO networks.**

## I. Introduction

Free space optics (FSO) have emerged as a promising technology for broadband wireless networks [1]. FSOs are wireless systems that use free space as transmission medium to transmit optical data signals at high bit rates. FSOs have many advantages such as cost effectiveness, long transmission distance, free license, interference immunity, high-bandwidth, among others. In recent years, considerable advances have been made in understanding the FSO channel, and both experimental data and commercial FSO transceivers are now available [1]. For widespread deployment of FSO networks, several important network problems should be addressed, such as how to design an FSO network topology with rich connectivity (making it robust to link failures) and how to accommodate traffic demands and QoS requirements of the underlying wired or wireless access network.

The FSO network topology design problem has been addressed in several prior works. In [2], a distributed Minimum Spanning Tree (MST) algorithm was proposed to build degree-bounded tree topologies. In [3], [4], algorithms were developed to maximize network connectivity and make a mesh topology. The load balancing problem was addressed in [5], [6], where several topology design heuristics were developed to minimize network-wide average load. To maximize the potential of FSO networks, the unique characteristics of FSO links should be considered in the formulation, and the problems of topology design and routing of the traffic flows should be jointly considered and optimized [5], [6]. Usually such problems are highly complex. However, an approximation algorithm with performance guarantees (i.e., in the form of a bounded *optimality gap*) would be highly appealing.

In this paper, we investigate the problem of joint topology design and load balancing in FSO networks, considering important design issues such as link reliability, cost constraints, traffic characteristics and demand, QoS requirements, routing policies, and network topology. We assume that a traffic matrix is known and the total number of edges used for building a topology is given a priori (e.g., due to cost constraint). We then formulate the joint topology design and load balancing problem with objectives to minimize the network-wide average load or network-wide average delay. Both short-range dependent (SRD) and long-range dependent (LRD) traffic models are considered in deriving the network delays.

With the objective function of average load, the formulated problem is a Mixed Integer Linear Programming (MILP) problem, while with the objective function of average delay, the formulated problem is a Mixed Integer Nonlinear Programming (MINLP) problem. These problems are NP-hard in general [5], [6]. In prior works [5], [6], effective heuristic algorithms were presented to minimize the network-wide average load. However, there was no guarantee on the optimality performance of these heuristics, and the algorithms do not apply to the more complex problem of minimizing network-wide average delay.

In this paper, we develop a Reformulation-Linearization Technique (RLT)-based branch-and-bound algorithm that can produce highly competitive solutions with bounded performance. RLT is a useful technique that can be applied to derive linear programming (LP) relaxations for an underlying non-linear non-polynomial programming problem [7]. We first adopt RLT to obtain LP relaxations for the complex MILP and MINLP problems. We then incorporate the LP relaxations into the branch-and-bound framework to compute (1-$\epsilon$)-optimal solutions, where $0 \leq \epsilon \ll 1$ is a prescribed tolerance. When the algorithm terminates, it produces a feasible solution to the original MILP or MINLP problem, which is within the $\epsilon$ range of the global optimum. The RLT-based branch-and-bound algorithm is evaluated with simulations, and is shown to be highly suitable for joint topology and load balancing optimization in FSO networks.

The remainder of this paper is organized as follows. In section II, we describe our network, channel, and performance models and assumptions, and formulate the optimization problem. The RLT-based algorithm is presented in Section III and its performance is evaluated in Section IV. Section V concludes the paper.

## II. SYSTEM MODEL AND PROBLEM STATEMENT

### A. Network Model

We consider an FSO network consisting of $n$ base stations (BS), which provide mobile users with network access. Each BS could be the head of a cluster consisting of multiple access points [4]. The aggregate traffic will be relayed through wireless optical links. We assume that each BS has multiple sets of wireless optical devices in order to support the aggregate traffic load and provide a rich mesh connectivity. The FSO links are immune to electromagnetic interference and are point-to-point connections with narrow beam divergence [1], [4]–[6].

The FSO network can be modeled as a *simple* graph $G(V, E)$, where each vertex $v \in V$ represents a BS and each edge $e \in E$ is an FSO link. Let $n$ and $m$ denote the cardinality of $V$ and $E$ respectively. We assume an $n \times n$ *traffic matrix* $\mathbf{F}$ that describes the traffic demand (measured, estimated, or projected) for the access network, where each element $f_{sd} = [\mathbf{F}]_{sd}$ represents the mean data rate between each source and destination pair $s$-$d$.

We characterize each FSO link $e = (i, j) \in E$ with two parameters: i) link capacity $c_{ij}$; and ii) link reliability $\gamma_{ij}$. As in prior work [6], we assume that each FSO channel is full duplex with symmetric capacity and a nominal data rate $c$ is achievable within a predefined transmission range, i.e., $c_{ij} = c_{ji} = c$ for all $i \neq j$. We also assume symmetric link reliability, i.e., $\gamma_{ij} = \gamma_{ji}$ for all $i \neq j$, due to the line-of-sight transmissions with narrow beam divergence. There is connectivity between two BS's if the link reliability is larger than a threshold $\gamma_{th}$.

### B. FSO Channel Model

We adopt the *log-normal* model to characterize FSO link reliability under turbulent atmosphere [8], [9]. The marginal distribution of light intensity fading induced by atmospheric turbulence can be statistically modeled as [8]

$$f_I(I) = \frac{1}{2\sigma_X I}\frac{1}{\sqrt{2\pi}}\exp\left\{-\frac{[\ln(I) - \ln(I_0)]^2}{8\sigma_X^2}\right\}, \quad (1)$$

where $\sigma_X^2$ is the variance and $I_0$ is the received average intensity without turbulence. The standard deviation $\sigma_X^2$ can be approximated as $\sigma_X^2 = 0.30545\,(2\pi/\lambda)^{7/6}\,C_n^2(L)z^{11/6}$, where $\lambda$ is the wavelength, $C_n^2(L)$ is the *index of refraction structure parameter* with constant altitude $L$, and $z$ is the distance. It is shown that for atmospheric channels near the ground (i.e., $L <$ 18.5m), $C_n^2$ ranges from $10^{-13}\mathrm{m}^{-2/3}$ to $10^{-17}\mathrm{m}^{-2/3}$ for strong and weak atmospheric turbulence respectively [8]. The common average is $10^{-15}\mathrm{m}^{-2/3}$.

The link reliability $\gamma_{ij}$ is the probability that the intensity of received signal $I$ exceeds a threshold $I_{th}$, which can be computed using the *error functin* $\mathrm{erf}(\cdot)$ as

$$\gamma_{ij} = P(I \geq I_{th}) = \frac{1}{2} - \frac{1}{2}\,\mathrm{erf}\left(\frac{\ln(I_{th}/I_0)}{2\sqrt{2}\sigma_X}\right). \quad (2)$$

The ratio $I_{th}/I_0$ can be interpreted as *transmittance* according to Beer-Lambert Law [10], which is determined by the distance and absorption coefficient. For a fixed ratio $I_{th}/I_0$, $\gamma_{ij}$ depends on the standard deviation $\sigma_X$, which is strongly influenced by weather conditions and transmission distance. We assume that the set of edges satisfying $\gamma_{ij} \geq \gamma_{th}$ forms the *candidate link set* for constructing the FSO network topology.

### C. Performance Measures

*1) Network-wide Average Load (L):* We adopt multipath routing for load balancing, where a flow $f_{sd}$ may be split into multiple subflows. Let $f_{ij}^{sd}$ be the subflow passing through a link $(i, j)$. We have the flow-conservation condition:

$$\sum_{j=1}^{n} f_{ij}^{sd} - \sum_{j=1}^{n} f_{ji}^{sd} = \begin{cases} f_{sd}, & i = s, \text{ for all } i \in V \\ -f_{sd}, & i = d, \text{ for all } i \in V \\ 0, & \text{otherwise, for all } i \in V. \end{cases} \quad (3)$$

Considering all the $s$-$d$ pairs, the average traffic load $\lambda_{ij}$ and the link utilization $\rho_{ij}$ at link $(i, j)$ are

$$\lambda_{ij} = \textstyle\sum_{s,d\in V} f_{ij}^{sd} \ \text{ and } \ \rho_{ij} = \lambda_{ij}/c_{ij} < 1. \quad (4)$$

For the link to be stable, we have $\rho_{ij} < 1$, for all $(i, j) \in E$. We define the *network-wide average load* $L$ as

$$L \cong (1/\lambda) \cdot \textstyle\sum_{(i,j)\in E} \lambda_{ij}, \quad (5)$$

where $\lambda = \sum_{s,d\in V} f_{sd}$, i.e., the sum of total traffic demands. Note that when a packet is forwarded, it is counted multiple times in $L$. When all the $s$-$d$ traffic are transmitted through direct links, $L$ achieves its minimum value $L_{min} = 1$.

*2) Network-wide Average Delay ($T_1$, $T_2$):* We model each link $(i, j) \in E$ as a general queueing system with average input rate $\lambda_{ij}$ and service capacity $c_{ij}$. The average delay incurred at the link depends on the traffic auto-correlation structure. When the traffic constantly exhibits *short-range dependent* (SRD) characteristics (e.g., VoIP traffic), we can model the link queueing delay with an exponential distribution with parameter $c_{ij} - \lambda_{ij}$ [11]. Applying Little's formula, the network-wide average delay $T_1$ can be computed as

$$T_1 \cong \textstyle\sum_{(i,j)\in E} \frac{1}{\lambda}\frac{\lambda_{ij}}{c_{ij} - \lambda_{ij}}. \quad (6)$$

When the traffic exhibits *long-range dependent* (LRD) characteristics (e.g., data traffic), we can model each link as a *fractional Brownian motion* (fBm) queueing system, where the queue length has a heavy-tailed *Weibull* distribution [12]

$$\Pr\{Q_{ij} > q\} \approx \exp\left\{-\frac{(c_{ij} - \lambda_{ij})^{2H}}{2\kappa^2(H)a\lambda_{ij}} q^{2-2H}\right\}, \quad (7)$$

where $\kappa(H) = H^H(1 - H)^{1-H}$, $H \in [0.5, 1)$ is the Hurst parameter, and $a$ is the index of dispersion. Applying Little's formula, the network-wide average delay $T_2$ is

$$T_2 \cong \frac{1}{\lambda}\Gamma\left(1 + \frac{1}{2-2H}\right)\textstyle\sum_{(i,j)\in E}\left[\frac{(c_{ij} - \lambda_{ij})^{2H}}{2\kappa^2(H)a\lambda_{ij}}\right]^{\frac{-1}{2-2H}}. \quad (8)$$

Defining $\tau = \frac{1}{\lambda}\Gamma(1+\frac{1}{2-2H})\left[2\kappa^2(H)a\right]^{\frac{1}{2-2H}}$, we have

$$T_2 = \tau \cdot \sum_{(i,j)\in E}\left[\lambda_{ij}/(c_{ij}-\lambda_{ij})^{2H}\right]^{\frac{1}{2-2H}}. \quad (9)$$

### D. Problem Statement

Without loss of generality, we consider the case of fixed BS's. The atmospheric condition can be known through weather forecast and past experiences. Then we can evaluate the edge reliabilities and determine the candidate edge set $\mathcal{E}_c$. The number of links in the FSO network is upper bounded by $m_c = |\mathcal{E}_c|$. The number of links is also lower bounded by $n-1$, the number of links that is needed to construct a connected network (i.e, a spanning tree).

The problem is to select $m$ links from $m_c$ candidate links to form a mesh topology. In addition, we also determine multipath routing for the $s$-$d$ flows, such that either the network-wide average load $L$ or the network-wide average delay $T_1$ or $T_2$ is minimized. Define the following index variables for each link $(i,j) \in V$ as

$$x_{ij} = \begin{cases} 1, & \text{if } (i,j)\in\mathcal{E}_c \\ 0, & \text{otherwise.}\end{cases} \quad y_{ij} = \begin{cases} 1, & \text{if } (i,j) \text{ is chosen} \\ 0, & \text{otherwise.}\end{cases}$$

We have $x_{ij} \geq y_{ij}$ for all $(i,j)\in V$. The problem of joint topology design and load balancing, denoted as Problem OPT-TDLB, can be formulated as:

$$\textbf{minimize} \quad L/T_1/T_2 \quad (10)$$

**subject to:**

$$\sum_{i=1}^{n}\sum_{j=i}^{n} x_{ij} = m_c, \sum_{i=1}^{n}\sum_{j=i}^{n} y_{ij} = m, \text{ for } i,j\in V \quad (11)$$

$$y_{ij} \leq x_{ij}, x_{ij} = x_{ji}, y_{ij} = y_{ji}, \text{ for } i,j\in V \quad (12)$$

$$\theta_i^l \leq \sum_{j=1}^{n} y_{ij} \leq \theta_i^u, \text{ for } i\in V \quad (13)$$

$$0 \leq f_{ij}^{sd} \leq y_{ij} f_{sd}, \text{ for } i,j,s,d\in V \quad (14)$$

$$\lambda_{ij} = \sum_{s,d\in V} f_{ij}^{sd} \leq c_{ij}, \text{ for } (i,j)\in\mathcal{E}_c \quad (15)$$

$$\text{flow conservation constraint (3)} \quad (16)$$

$$x_{ij}\in\{0,1\}, y_{ij}\in\{0,1\}, \text{ for } i,j\in V. \quad (17)$$

In Problem OPT-TDLB, the optimization variables include binary variables $\mathbf{y} = \{y_{ij} \mid \forall\ i,j\in V\}$ and continuous variables $\mathbf{f} = \{f_{ij}^{sd} \mid \forall\ i,j,s,d\in V\}$. With objective function $L$, Problem OPT-TDLB($L$) is an MILP problem. With objective function $T_1$ or $T_2$, the corresponding Problems OPT-TDLB($T_1$) and OPT-TDLB($T_2$) are MINLP problems. Constraints (11) $\sim$ (13) are for edge selection and topology design, while constraints (14) $\sim$ (16) are for multipath routing and load balancing. In (13), $\theta_i^u$ is the maximum degree (enforced by some cost constraints), and $\theta_i^l$ is the minimum degree for BS $i$, which is required to support the incoming and outgoing traffic from the BS, as

$$\theta_i^l = \max\left\{\lceil\sum_{d=1}^{n}\lambda_{id}/c\rceil, \lceil\sum_{s=1}^{n}\lambda_{si}/c\rceil\right\}. \quad (18)$$

## III. RLT and Branch-and-Bound Algorithm

Our solution procedure for Problem OPT-TDLB is to incorporate an LP relaxation of the original problem into a branch-and-bound framework [7]. Problem OPT-TDLB($L$) is an MILP. We can obtain its LP relaxation by allowing the binary variables $y_{ij}$ to take real values in [0, 1]. In this section, we reformulate and linearize MINLP problems OPT-TDLB($T_1$) and OPT-TDLB($T_2$). The LP relaxations will then be incorporated into a branch-and-bound algorithm that can compute (1-$\epsilon$)-optimal solutions.

### A. Reformulation and Linearization: OPT-TDLB($T_1$)

To linearize the objective function $T_1$, we define substitution variables $t'_{ij}$ as $t'_{ij} = \lambda_{ij}/(c_{ij}-\lambda_{ij})$. Then we obtain a linear objective function $\sum t'_{ij}$ and additional nonlinear constraints $t'_{ij}\cdot c_{ij} - t'_{ij}\cdot\lambda_{ij} - \lambda_{ij} = 0$.

We next linearize the nonlinear constraint by defining substitution variables for the quadratic term $\mu_{ij} = t'_{ij}\cdot\lambda_{ij}$. Substituting $\mu_{ij}$ into the additional nonlinear constraints, we make them linear, but with the following additional *RLT bound-factor product constraints* for the new variable $\mu_{ij}$. Since $t'_{ij}$ and $\lambda_{ij}$ are bounded by their respective lower and upper bounds as $0 \leq t'_{ij} \leq \bar{t}'$ and $0 \leq \lambda_{ij} \leq c_{ij}$, we have

$$\begin{cases} (t'_{ij}-0)\cdot(\lambda_{ij}-0) \geq 0 \\ (t'_{ij}-0)\cdot(c_{ij}-\lambda_{ij}) \geq 0 \\ (\bar{t}'-t'_{ij})\cdot(\lambda_{ij}-0) \geq 0 \\ (\bar{t}'-t'_{ij})\cdot(c_{ij}-\lambda_{ij}) \geq 0. \end{cases} \quad (19)$$

Expanding (19) and substituting $\mu_{ij} = t'_{ij}\cdot\lambda_{ij}$, we obtain the following RLT constraints:

$$\begin{cases} \mu_{ij} \geq 0 \\ c_{ij}\cdot t'_{ij} - \mu_{ij} \geq 0 \\ \bar{t}'\cdot\lambda_{ij} - \mu_{ij} \geq 0 \\ \bar{t}'\cdot c_{ij} - c_{ij}\cdot t'_{ij} - \bar{t}'\cdot\lambda_{ij} + \mu_{ij} \geq 0. \end{cases} \quad (20)$$

Therefore we obtain an LP relaxation $l$-OPT-TDLB($T_1$) as

$$\textbf{minimize} \quad (1/\lambda)\cdot\sum_{(i,j)\in E} t'_{ij} \quad (21)$$

**subject to:**

$$\text{constraints (11)} \sim \text{(16)} \quad (22)$$

$$0 \leq y_{ij} \leq 1, \text{ for } (i,j)\in\mathcal{E}_c \quad (23)$$

$$c_{ij}\cdot t'_{ij} - \mu_{ij} - \lambda_{ij} = 0, \text{ for } (i,j)\in\mathcal{E}_c \quad (24)$$

$$\text{RLT bound-factor constraints (20) for } (i,j)\in\mathcal{E}_c. \quad (25)$$

### B. Reformulation and Linearization: OPT-TDLB($T_2$)

The objective function $T_2$ consists of exponents. We define substitution variables for the exponents as $t''_{ij} = \left[\lambda_{ij}/(c_{ij}-\lambda_{ij})^{2H}\right]^{1/(2-2H)}$. Substituting $t''_{ij}$ we obtain a linear objective function $\tau\sum t''_{ij}$, along with additional nonlinear constraints: $t''_{ij}\cdot(c_{ij}-\lambda_{ij})^{\frac{H}{1-H}} - \lambda_{ij}^{\frac{1}{2-2H}} = 0$. Letting $\nu_{ij} = c - \lambda_{ij}$, we have $t''_{ij}\cdot(\nu_{ij})^{\frac{H}{1-H}} - \lambda_{ij}^{\frac{1}{2-2H}} = 0$. Finally, taking logarithms and defining substituting variables

$$\zeta_{t''_{ij}} = \log(t''_{ij}),\ \ \zeta_{\lambda_{ij}} = \log(\lambda_{ij}),\ \ \zeta_{\nu_{ij}} = \log(\nu_{ij}), \quad (26)$$

we obtain linear constraints $\zeta_{t''_{ij}} - \frac{1}{2-2H}\zeta_{\lambda_{ij}} + \frac{H}{1-H}\zeta_{\nu_{ij}} = 0$.

We still need to linearize the new nonlinear constraints (26), which are all in the form of $y = \log(x)$. If $x$ is bounded by $0 < x_l \leq x \leq x_u$, the logarithm relationship can be linearized

This full text paper was peer reviewed at the direction of IEEE Communications Society subject matter experts for publication in the IEEE Globecom 2010 proceedings.

using a *polyhedral outer approximation* comprised of a convex envelop in concert with several tangential supports [7], i.e.,

$$\begin{cases} y \geq \frac{\log(x_u)-\log(x_l)}{x_u-x_l} \cdot (x-x_u)+\log(x_u) \\ y \leq x/x_k+\log(x_k)-1, \end{cases} \quad (27)$$

where $x_k = x_l + \frac{k}{k_{max}-1}(x_u - x_l)$ for $k = 0, \cdots, k_{max}-1$. The convex envelope consists of a chord connecting two end points and $k_{max}$ supports each being tangent to the log(x) curve at $x_k$. Therefore, we generate $(k_{max}+1)$ new linear constraints for each logarithmic substitution variables.

Therefore we obtain an LP relaxation $l$-OPT-TDLB($T_2$) as

$$\textbf{minimize} \quad \tau \cdot \textstyle\sum_{(i,j)\in E} t''_{ij} \quad (28)$$

**subject to:**

$$\text{constraints (11)} \sim \text{(16)} \quad (29)$$

$$0 \leq y_{ij} \leq 1, \ \text{for } (i,j) \in \mathcal{E}_c \quad (30)$$

$$\zeta_{t''_{ij}} - \frac{1}{2-2H}\zeta_{\lambda_{ij}} + \frac{H}{1-H}\zeta_{\nu_{ij}} = 0, \ \text{for } (i,j) \in \mathcal{E}_c \quad (31)$$

$$\nu_{ij} + \lambda_{ij} = c_{ij}, \ \text{for } (i,j) \in \mathcal{E}_c \quad (32)$$

polyhedral outer approximations (27) for

$$\zeta_{t''_{ij}}, \zeta_{\lambda_{ij}}, \zeta_{\nu_{ij}} \text{ given in (26), for } (i,j) \in \mathcal{E}_c. \quad (33)$$

### C. Branch-and-Bound Algorithm

In this section, we embedded the LP relaxations into the branch-and-bound framework to obtain solutions with bounded optimality gap. Branch-and-bound is an iterative optimization algorithm that is especially useful for solving discrete and combinatorial problems. It consists of two key components: (i) a strategy to split a problem into subproblems with smaller sizes, i.e., *branching*, and (ii) a fast way to obtain lower and upper bounds (LB, UB) for the subproblems, i.e., *bounding*. The resulting subproblems forms a tree structure, while the set of leaf nodes is called *problem list* P. During the solution process, a branch of the tree may be deleted (or, *fathomed*) from future search, if all its solutions are dominated by some other subproblems, therefore reducing the computational cost.

Our RLT-based Branch-and-Bound algorithm is given in Table I. Solving the LP relaxation $l$-OPT-TDLB with an LP solver can provide an infeasible solution $\hat{\delta} = (\hat{\mathbf{y}}, \hat{\mathbf{f}})$ and an LB for the original problem. Then we apply a *local search* algorithm to derive a feasible solution $\delta$ in the neighborhood of $\hat{\delta}$, which provides an UB for the original problem. The global LB and UB are updated as follows:

$$\begin{cases} \text{LB} = \min\{\text{LB}_h : \text{all problems } h \in \text{P}\} \\ \text{UB} = \min\{\text{UB}_h : \text{all problems } h \in \text{P}\}. \end{cases} \quad (34)$$

We adopt a simple local search algorithm that first determines the network topology (i.e., fixing the $y_{ij}$'s to binaries). According to constraint (11), $m$ links should be selected from the candidate set $\mathcal{E}_c$ to form a topology. Hence, we choose the $m$ largest $\hat{y}_{ij}$'s in $\mathbf{y}$ and set them to 1; the rest smaller $\hat{y}_{ij}$'s are set to 0. When the topology is fixed, we determine the optimal multipath routing by solving Problem $l$-OPT-TDLB again for the $f_{ij}^{sd}$'s. The resulting solution $\delta = (\mathbf{y}, \mathbf{f})$ is thus feasible and provides an upper bound.

TABLE I
BRANCH-AND-BOUND ALGORITHM FOR PROBLEM OPT-TDLB.

<u>Initialization</u>:
  Initialize $\delta^* = \emptyset$ and UB = $\infty$;
  Initialize problem list P with the original Problem 1;
  Relaxation:
    Obtain $l$-OPT-TDLB for Problem 1;
    Solve $l$-OPT-TDLB to obtain solution $\hat{\delta} = (\hat{\mathbf{y}}, \hat{\mathbf{f}})$ and the
    objective value as the lower bound LB$_1$;
<u>Iteration</u>:
  Select problem $h$ with the minimum LB$_h$ from P
  Set LB=LB$_h$ and let $\hat{\delta}$ be its relaxed solution;
  Local Search:
    Obtain feasible solution $\delta$ from $\hat{\delta}$ with the local search alg.;
    Compute UB$_h$ from $(\mathbf{y}, \mathbf{f})$;
  If (UB$_h$ < UB)
    Update $\delta^* = \delta$ and UB = UB$_h$;
    If LB $\geq (1-\epsilon) \cdot$ UB, stop with $(1-\epsilon)$-solution $\delta^*$;
    Otherwise, discard all problems $h'$ from P satisfying
    LB$_h \geq (1-\epsilon)\cdot$ UB;
  Partition:
    Find $\tilde{y}_{ij}$ which is closest to 1 but not fixed yet;
    Split problem $h$ into $h_1$ and $h_2$ with respect to $\tilde{y}_{ij}$;
  Bounding:
    Solve the RLT relaxations of the two subproblems and obtain
    their lower bounds LB$_{h_1}$ and LB$_{h_2}$;
  Remove problem $h$ from P;
  If LB$_{h_1} < (1-\epsilon)\cdot$ UB, insert problem $h_1$ into P;
  If LB$_{h_2} < (1-\epsilon)\cdot$ UB, insert problem $h_2$ into P;
  If P = $\emptyset$, stop with current best solution, $\delta^*$;
  Otherwise, enter the next iteration;

For branching, we choose the subproblem $h$ with the smallest LB$_h$, which is indicative of the global optimal solutions. Subproblem $h$ is then partitioned into two subproblems, $h_1$ and $h_2$, which replace the subproblem $h$ in P. The corresponding LB$_{h_1}$, LB$_{h_2}$, UB$_{h_1}$, and UB$_{h_2}$ are calculated, and the global LB and UB are updated as in (34). The iteration procedure terminates when there is a feasible solution satisfying LB $\geq (1-\epsilon) \cdot$ UB, or when the problem list P is empty.

## IV. SIMULATION STUDIES

### A. Simulation Setting

In the simulations, $n$ BS's are randomly deployed in a rectangular region. We present simulation results for the cases $n = 5$ and $n = 7$. Assume the traffic matrix $\mathbf{F}$ is given, which is randomly generated for the $s$-$d$ pairs [6]. Each $s$-$d$ flow $f_{sd}$ ranges from 0 to 40% of the FSO link capacity. The constraints of minimum node degrees are determined from $\mathbf{F}$ as in (18).

Link connectivity is determined by the link reliability, which is derived using the FSO channel model given in Section II-B. Then the $x_{ij}$ are known and the the candidate link set $\mathcal{E}_c$ is found. We use reliability threshold $\gamma_{th} = 99.99\%$ when determining the candidate set. For LRD traffic model, the index of dispersion $a$ is set to a half of the link capacity and Hurst parameter $H$ is chosen to be 0.7.

The proposed solution procedure is implemented in MATLAB ver 7.4.0 for manipulating matrices and solving the LP relaxations. The codes are executed on a standard PC with a Core Duo 2.20 GHz processor and 2 GB memory.

978-1-4244-5638-3/10/$26.00 ©2010 IEEE

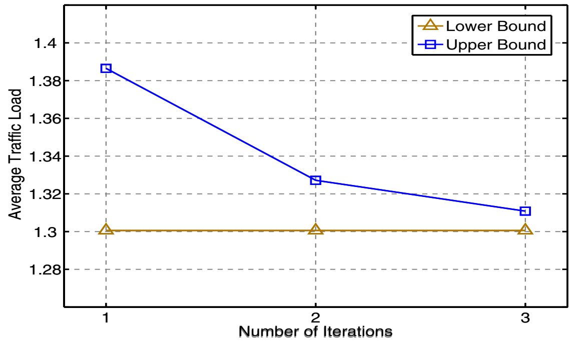


(a) OPT-TDLB($L$) with SRD traffic, gap = 0.78%

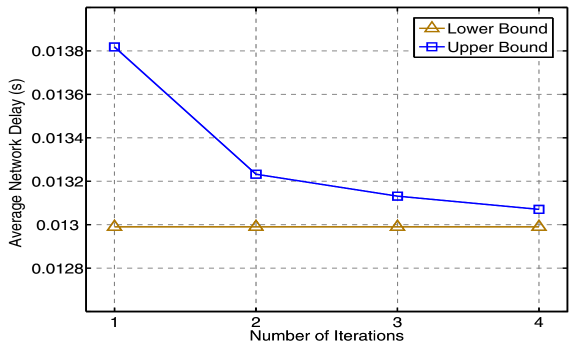


(b) OPT-TDLB($T_1$), gap = 0.62%

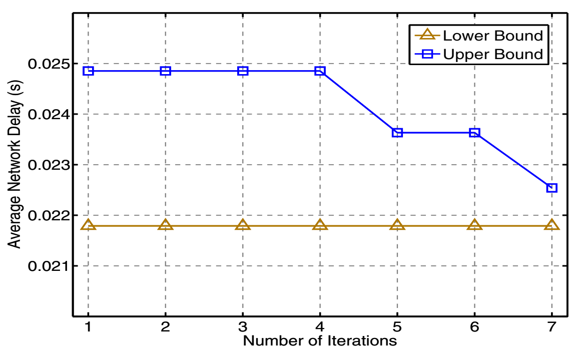


(c) OPT-TDLB($T_2$), gap = 3.33%

Fig. 1. Convergence of the branch-and-bound algorithm for the 5-node network with optimality gap $\epsilon = 0.01, 0.01$, and 0.07, respectively.

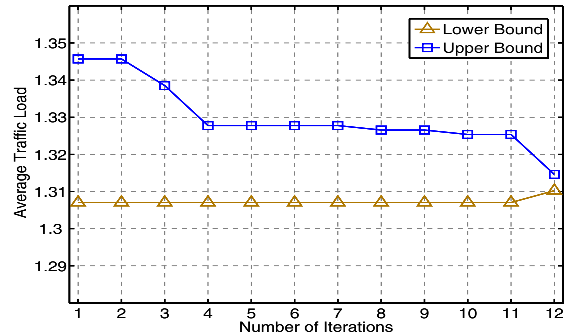


(a) OPT-TDLB($L$) with SRD traffic, gap = 0.33%

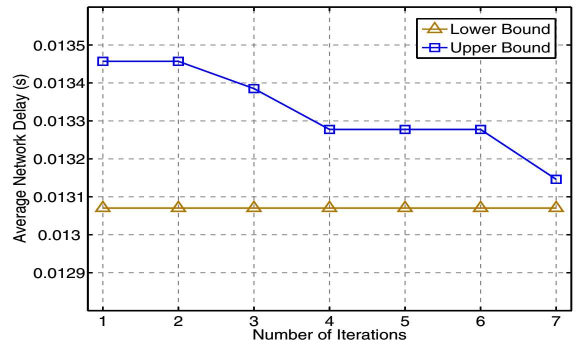


(b) OPT-TDLB($T_1$), gap = 0.58%

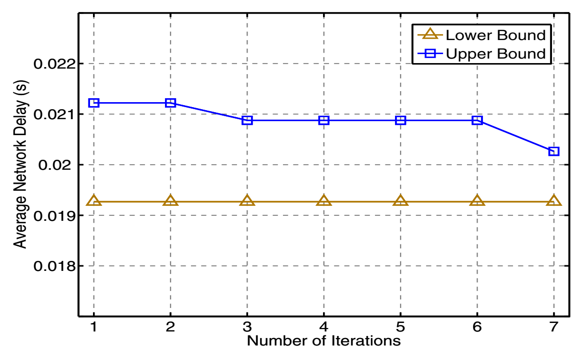


(c) OPT-TDLB($T_2$), gap = 4.91%

Fig. 2. Convergence of the branch-and-bound algorithm for the 7-node network with optimality gap $\epsilon = 0.01, 0.01$, and 0.07, respectively.

### *B. Convergence and Optimality Gap*

The branch-and-bound algorithm can provide $(1 - \epsilon)$-optimal solution. That is, the feasible solution it produces is within the $\epsilon$ range of the global optimal solution. We first examine the convergence and the final optimality gap achieved by the proposed algorithm.

In Fig. 1, we plot the simulation results for the 5-node FSO network. We use the branch-and-bound algorithm to solve the three variations of Problem OPT-TDLB, i.e., Problem OPT-TDLB($L$) with SRD traffic, Problem OPT-TDLB($T_1$), and Problem OPT-TDLB($T_2$). The termination criteria are chosen to be $\epsilon$ = 0.01, 0.01, 0.07 for the three problems, respectively. The simulations terminate when LB $\geq (1 - \epsilon) \cdot$ UB, and the upper bounding solution is a feasible one. The Problem OPT-TDLB($L$) results are shown in Fig. 1(a), where the proposed algorithm terminates after three iterations and achieves an optimality gap of 0.78%. The Problem OPT-TDLB($T_1$) results are shown in Fig. 1(b), where the algorithm terminates after four iterations and achieves a 0.62% optimal gap. In the case of Problem OPT-TDLB($T_2$), the algorithm terminates after seven iterations (due to the high variation in LRD traffic and the need to handle logarithm functions) with a 3.33% optimality gap, as shown in Fig. 1(c).

In Fig 2, we show convergence and optimality gap results for the 7-node FSO network. The proposed algorithm takes slightly more iterations to finish, due to increased network size. For Problem OPT-TDLB($L$), the algorithm takes 12 iterations to achieve an optimal gap of 0.33% (see Fig. 2(a)). For Problem OPT-TDLB($T_1$), the algorithm takes seven iterations to achieve an optimality gap of 0.58%, as shown in Fig. 2(b). For Problem OPT-TDLB($T_1$), the algorithm takes seven iterations

TABLE II
AVERAGE BUILDING AND EXECUTION TIME PER SUBPROBLEM FOR THE BRANCH-AND-BOUND ALGORITHM

| Problem Type | Size of $\mathbf{Q}$ | Size of $\mathbf{Q}_{eq}$ | Average Building Time (sec) | Average Execution Time (sec) |
|---|---|---|---|---|
| $l$-OPT-TDLB($L$), LB, 5 nodes | 425 × 440 | 131 × 440 | 0.835 | 0.710 |
| $l$-OPT-TDLB($L$), UB, 5 nodes | n/a | 112 × 252 | 0.018 | 0.036 |
| $l$-OPT-TDLB($T_1$), LB, 5 nodes | 445 × 480 | 151 × 480 | 1.075 | 0.219 |
| $l$-OPT-TDLB($T_1$), UB, 5 nodes | 12 × 276 | 124 × 276 | 0.024 | 0.042 |
| $l$-OPT-TDLB($T_2$), LB, 5 nodes | 733 × 540 | 159 × 540 | 4.518 | 0.242 |
| $l$-OPT-TDLB($T_2$), UB, 5 nodes | 216 × 312 | 136 × 312 | 0.140 | 0.091 |
| $l$-OPT-TDLB($L$), LB, 7 nodes | 1,813 × 1,848 | 358 × 1,848 | 85.067 | 7.995 |
| $l$-OPT-TDLB($L$), UB, 7 nodes | n/a | 318 × 1,032 | 1.296 | 0.081 |
| $l$-OPT-TDLB($T_1$), LB, 7 nodes | 1,855 × 1,932 | 400 × 1,932 | 93.516 | 8.963 |
| $l$-OPT-TDLB($T_1$), -UB, 7 nodes | 24 × 1,080 | 342 × 1,080 | 1.613 | 0.089 |
| $l$-OPT-TDLB($T_2$), LB, 7 nodes | 2,543 × 2,058 | 436 × 2,058 | 184.305 | 14.110 |
| $l$-OPT-TDLB($T_2$), UB, 7 nodes | 432 × 1,152 | 366 × 1,152 | 4.823 | 0.281 |

to achieve an optimality gap of 4.91%.

### C. Computational Cost

We next present the computation cost results in the form of execution time of the proposed algorithm, which largely depends on the efficiency of the underlying LP solver on handling large matrices. Since the algorithm is an iterative one, we focus on the execution time per iteration for clarity.

In Table II, the average parameter building time (i.e., the time spent on obtaining the LP relaxations and assembling the input matrices to the LP solver) and the average execution time (i.e., the time it takes for the LP solver to solve the relaxed problem) for solving one sub-problem in the Problem List P are listed. In the table, $\mathbf{Q}$ and $\mathbf{Q}_{eq}$ are matrix inputs to the LP solver, whose sizes largely depend on the number of constraints of the LP relaxation $l$-OPT-TDLB.

We find that the building and execution times are proportional to the parameter matrix sizes. To compute the LB for a subproblem, the corresponding LP relaxation, $l$-OPT-TDLB, should be solved to determine the topology design variables $\mathbf{y}$ and the multipath routing variables $\mathbf{f}$. The constraints for $f_{ij}^{sd}$'s have more impact on the matrix sizes, due to new linear constraints introduced during the reformulation and linearization procedure for the objective functions. Once the lower-bounding solution $\hat{\delta}$ is found, it takes negligible time for the local search algorithm to find an upper-bounding solution $\hat{\delta}$ in the neighborhood, since the topology is already given in $\hat{\delta}$. For example, the average execution time is approximately 14 s to get the LB for a subproblem of $l$-OPT-TDLB($T_2$), while it only takes 0.3 s to obtain the UB for the subproblem.

From these simulation studies, we find that the branch-and-bound algorithm can produce feasible solutions that are highly competitive, as indicated by the very small optimality gaps when the algorithm terminates. Although the global optimum is unknown, the guarantee on the optimality gap ensures that the solutions are near-optimal. The threshold $\epsilon$ provides a convenient handle for the trade-off between computation time and optimality of the solution. These are useful features for the design and control of FSO networks.

## V. CONCLUSION

In this paper, we studied problem of joint topology design and load balancing in FSO networks. For a given traffic matrix, the objective is to design the topology and multipath routing policies for end-to-end flows, such that network-wide average load or network-wide average delay can be minimized. We developed effective branch-and-bound algorithm based on RLT for the formulated MILP and MINLP problems, which can provide highly competitive solutions with guaranteed performance. The efficacy of the proposed algorithm is validated with our simulation studies.

## ACKNOWLEDGMENT

This work is supported in part by the NSF under Grants ECCS-0802113, IIP-0738088 and IIP-1032002.

## REFERENCES

[1] V. W. Chan, "Free-space optical communications," *IEEE/OSA J. Lightw. Technol.*, vol. 24, no. 12, pp. 4750–4762, Dec. 2006.
[2] F. Liu, U. Vishkin, and S. Milner, "Bootstrapping free-space optical networks," *IEEE J. Sel. Areas Commun.*, vol. 24, no. 12, pp. 13–22, Dec. 2006.
[3] P. C. Gurumohan and J. Hui, "Topology design for free space optical networks," in *Proc. IEEE ICCCN'03*, Oct. 2003, pp. 576–579.
[4] I. K. Son and S. Mao, "Design and optimization of a tiered wireless access network," in *Proc. IEEE INFOCOM'10*, San Diego, CA, Mar. 2010.
[5] A. Desai and S. Milner, "Autonomous reconfiguration in free-space optical sensor networks," *IEEE J. Sel. Areas Commun.*, vol. 23, no. 8, pp. 1556–1563, Aug. 2005.
[6] A. Kashyap, K. Lee, M. Kalantari, S. Khuller, and M. Shayman, "Integrated topology control and routing in wireless optical mesh networks," *Computer Networks*, vol. 51, no. 15, pp. 4237–4251, 2007.
[7] S. Kompella, S. Mao, Y. Hou, and H. Sherali, "On path selection and rate allocation for video in wireless mesh networks," *IEEE/ACM Trans. Netw.*, vol. 17, no. 1, pp. 212–224, Feb. 2009.
[8] X. Zhu and J. M. Kahn, "Free-space optical communication through atmospheric turbulence channels," *IEEE Trans. Commun.*, vol. 50, no. 8, pp. 1293–1300, Mar. 2003.
[9] M. Al-Habash, L. Andrews, and R. Philips, "Mathematical model for the irradiance probability density function of a laser beam propagating through turbulent media," *Society of Photo-Optical Instrumentation Engineers*, vol. 40, no. 8, pp. 1554–1562, Aug. 2001.
[10] A. Prokes, "Atmospheric effects on availability of free space optics systems," *Optical Engineering*, vol. 48, no. 6, p. 066001, June 2009.
[11] D. Bertsekas and R. Gallager, *Data Networks*. Prentice Hall, 1992.
[12] I. Norros, "On the use of fractional brownian motion in the theory of connectionless networks," *IEEE J. Sel. Areas Commun.*, vol. 13, no. 6, pp. 953–962, Aug. 1995.